Effect of Supramicron Roughness Characteristics Produced by 1- and 2-step Acid Etching on the Osseointegration Capability of Titanium

Wael Att, DDS, Dr Med Dent[1]/Naoki Tsukimura, DDS, PhD[1]/Takeo Suzuki, DDS[2]/Takahiro Ogawa, DDS, PhD[3]

Purpose: *The purpose of this study was to compare the osteoblastic and osteogenic responses to titanium surfaces roughened by 1-step and 2-step acid etching.* ***Materials and Methods:*** *Titanium surfaces created by 1-step (AE1) and 2-step (AE2) acid-etching processes were analyzed using scanning electron microscopy (SEM), atomic force microscopy (AFM), and an optical interferometry (OI). Rat bone marrow–derived osteoblastic cells were cultured on these 2 surfaces. Cell proliferation was evaluated by counting the cells, while gene expression was analyzed using a reverse transcriptase-polymerize chain reaction. The biomechanical establishment of osseointegration was assessed via an in vivo implant push-in test in rat femurs. Additionally, the 2 surfaces were evaluated for their mechanical interlocking capability by a push-out test of titanium rods embedded in a resin block.* ***Results:*** *AFM analysis on a small scale of 5 μm × 5 μm showed that the 2 surfaces were similar in topography, having comparable micron-level roughness. However, larger scale (1000 μm × 1000 μm) SEM and OI analyses revealed that the AE1 surface consisted of supramicron convexity structures ranging from 10 μm to 50 μm in size, while the AE2 was relatively flat. No differences were found between the 2 surfaces in regard to the number of the cells proliferated or the expression of the bone-related genes. The biomechanical fixation of implants at week 2 was 22.2 ± 10.94 N and 25.4 ± 4.56 N for AE1 and AE2, respectively, with no significant difference between the 2 groups. The in vitro push-out values were 26.8 ± 7.85 N and 25.4 ± 8.56 N for AE1 and AE2, respectively, with no significant difference between the 2 groups.* ***Conclusion:*** *The different acid-etching procedures of titanium created similar micron-scale roughness profiles but distinct supramicron roughness characteristics. Osteoblastic function and in vivo osseointegration capacity, however, were not affected by this difference between the surfaces.*
INT J ORAL MAXILLOFAC IMPLANTS 2007;22:719–728

Key words: *bone-titanium integration, dental implants, osteoconduction, push-in test, surface topography*

Titanium is a biocompatible material that is used extensively for the fabrication of dental and orthopedic implants. Numerous studies have demonstrated the osteoconductive properties of titanium, which lead to bone-implant anchorage or osseointegration.[1,2] Implant surface topography is one of several factors critical to successful osseointegration.[3,4]

The degree of roughness and the orientation of surface irregularities are important topographical properties of implant surfaces.[5] Numerous additive and subtractive techniques have been introduced to alter the surface topography of implants, such as oxidizing, sandblasting, acid etching, and combinations of these techniques.[6] The ultimate goal of such surface modifications is to achieve superior peri-implant osteogenesis than that around dental implants with conventional surfaces, such as machined or titanium plasma-sprayed (TPS) surfaces. Implant surfaces having a micron-scale topographic configuration, or microroughened surfaces, have been shown to give rise to a particular fibrin retention that allows osteogenic cells to migrate to the implant surface,

[1]Visiting Research Professor, The Jane and Jerry Weintraub Center for Reconstructive Biotechnology, Division of Advanced Prosthodontics, Biomaterials and Hospital Dentistry, UCLA School of Dentistry, Los Angeles, California.
[2]Visiting Scholar, The Jane and Jerry Weintraub Center for Reconstructive Biotechnology, Division of Advanced Prosthodontics, Biomaterials and Hospital Dentistry, UCLA School of Dentistry, Los Angeles, California.
[3]Professor, The Jane and Jerry Weintraub Center for Reconstructive Biotechnology, Division of Advanced Prosthodontics, Biomaterials and Hospital Dentistry, UCLA School of Dentistry, Los Angeles, California.

Correspondence to: Dr Wael Att, The Jane and Jerry Weintraub Center for Reconstructive Biotechnology, Division of Advanced Prosthodontics, Biomaterials and Hospital Dentistry, Box 951668, CHS B3-087, Los Angeles, CA 90095-1668. Fax: +1 310 825 6345. E-mail: waelatt@ucla.edu

enhance the expression pattern of osteoblastic genes and provide rapid maturation of osteoblasts and faster mineralization of the extracellular matrix.[7–9] In vivo, these microroughened implant surfaces show an increased percentage of bone-to-implant contact compared to machined surfaces.[10] Furthermore, these implants typically require higher forces to break implant-bone anchorage than so-called smooth implants.[8,11,12] However, whether the increased mechanical stability of microroughened implants is due to increased mechanical locking of tissue within the surface roughness, increased bone-implant contact, increased quantity and quality of surrounding bone, or a combination of these features, is still debatable.[13–15] Despite significant improvements in implant surface modifications, no specific surface has consistently been associated with better clinical outcomes than other surfaces.[5]

A review of current systems found that most implant surfaces are fabricated by either a 1-step processing such as oxidizing, sandblasting, or acid etching (using single or a mixture of acids) or a 2-step processing like sandblasting followed by acid etching or double acid etching.[6] The resultant surface morphology can include alterations of the implant surface at the micrometer level of resolution (high-frequency structures, such as micropits) or the supra-micron level of resolution (low-frequency structures, such as waves, or macroirregularities) or both.[16] For example, titanium surface sandblasting prior to acid etching may provide macroroughness (changes in the surface ranging from 20 to 40 µm in diameter) before microroughness is created by acid-etching.[16,17] However, the means through which the structural combination of micron-roughness (high-frequency structures) and supra-micron roughness (low-frequency structures) affects the behavior and response of osteoblasts, and eventually the osseointegrative capacity of titanium surfaces, is unknown.[18,19]

Microroughened surfaces with or without supramicron roughness have been successfully created via a relatively simple modification of the acid-etching procedure. One-step acid etching with sulfuric acid produced a combination of micro- and supra-microroughness, while 2-step acid-etching with hydrofluoric acid and sulfuric acid produced only a microroughened surface. Although these surfaces do not feature surface topographies identical to those of commercially available implants, these surfaces may be a useful model to study the biological effects of different supramicron roughness characteristics. The purpose of this study was to examine the osteoblastic function and biomechanical establishment of osseointegration responding to microroughened titanium surfaces with or without supramicroroughness.

MATERIALS AND METHODS

Titanium Samples and Surface Characterization

Machine turned, commercially-pure grade 2 titanium disks with a diameter of 20 mm were divided into 2 test groups according to the acid-etching technique used: the 1-step acid-etching group (AE1) and the 2-step acid-etching group (AE2). The disks of group AE1 were prepared by acid etching with 67% (w/w) sulfuric acid (H_2SO_4) at 120°C for 75 seconds. Disks from group AE2 were acid etched with 20% hydrofluoric acid for 30 seconds, followed by 67% sulfuric acid at 120°C for 75 seconds. The disks of both groups were then washed twice using double-distilled water, dried, and stored in an airtight container. Using the aforementioned techniques, 20 unthreaded cylindric titanium rods were acid etched and divided into 2 groups of 10 implants each (AE1 and AE2). The dimensions of the titanium cylinders were measured using a precise thickness-measuring device (Digimatic Micrometer; Mitsutoyo, Hamamatsu, Japan). The AE1 cylinders had an average diameter of 1.142 ± 0.007 mm and an average length of 1.980 ± 0.017 mm, while the AE2 group had an average diameter of 1.113 ± 0.003 mm and an average length of 1.980 ± 0.011 mm, with no statistical differences between the 2 implants ($P > .05$).

The topographic appearance of the 2 surfaces was examined using scanning electron microscopy (SEM, Stereoscan 250, Cambridge Company, Cambridge, MA). Further qualitative and quantitative examinations of the surface topography were performed via atomic force microscopy (EDX, SPM-900J3, Shimadzu, Japan) for smaller-scale analysis of areas 5 µm × 5 µm and via an optical interferometer (OI) equipped with a surface-mapping microscope (MicroXAM 100; ADE Phase Shift, Tucson, AZ) for analyzing larger areas of 1,000 µm × 1,000 µm. Fourier analysis was used to calculate average roughness (R_a), root-mean-square roughness (R_{rms}), peak-to-valley ($R_{p\text{-}v}$) and interirregularity space (Sm) values. To further quantify the horizontal profile of the surfaces, the density of convexity was manually measured. The convexity was defined as a structure consisting of a peak or peaks whose height was greater than 3 µm in the topographical profile in the OI analysis, and the number of convexities in a cross section of 1,000 µm width was counted. For these surface topographical variables, 4 independent samples per group were analyzed and averaged.

The surfaces of the 2 test groups were also examined by an energy dispersive x-ray spectrometer (EDX, JSM-5900LV, Joel, Tokyo, Japan) for elemental composition and by x-ray diffraction (XRD, Rad-rC, Rigaku, Tokyo, Japan) for determining crystalline properties using Cu-Kα radiation (40 kV and mA).

Table 1 Primer Design and Condition for PCR

Target gene	Forward primer	Backward primer	Annealing temperature	No. of cycles	Size of PCR products (bp)
Collagen I	5'-GGCAACAGTCGATTCACC-3'	5'-AGGGCCAATGTCCATTCC-3'	58	28	177
Osteopontin	5'-GATTATAGTGACACAGAC-3'	5'-AGCAGGAATACTAACTGC-3'	45	19	443
Osteocalcin	5'-GTCCCACACAGCAACTCG-3'	5'-CCAAAGCTGAAGCTGCCG-3'	61	25	193
GAPDH	5'-TGAAGGTCGGTGTCAACGGATTTGGC-3'	5'-CATGTAGGCCATGAGGTCCACCAC-3'	67	27	983

bp = base pairs.

Osteoblastic Cell Culture

Bone marrow cells were obtained from the femurs of 8-week-old Sprague-Dawley rats. After the animals were sacrificed, the femurs were aseptically removed and cleaned from the attached muscles and ligaments. After the bones had been washed with 1% phosphate buffer solution (PBS; MP Biomedicals, Solon, OH) and metaphyses had been removed from both ends, the bone marrow cavity was flushed out with alpha-modified Eagle's medium supplemented with 15% fetal bovine serum, 50 µg/mL ascorbic acid, 10 mmol/L Na-β-glycerophosphate, 10^{-8} dexamethasone, and antibiotic-antimycotic solution containing 10,000 units/mL penicillin G sodium, 10,000 mg/mL streptomycin sulfate and 25 mg/mL amphotericin B. The cells were incubated in a humidified atmosphere of 95% air, 5% CO_2 at 37°C. At 80% confluency, the cells were detached using 0.25% Trypsin-1 mmol/L EDTA-4Na and seeded onto titanium disks for both test groups at a density of 4×10^4 cells/cm^2. The cells were cultured for up to 14 days, and the medium was renewed every 3 days.

Cell Density Assay

At culture days 3 and 5, the cells were gently rinsed twice with PBS and treated with 0.1% collagenase in 300 µL of 0.25% trypsin-1 mmol/L EDTA-4Na for 15 minutes at 37°C. A hematocytometer was used to count the number of detached cells obtained from 3 wells per experimental group. SEM was used for the selected culture to confirm the absence of any cell remnant on the substrates. Three independent cultures were analyzed for each group.

Gene Expression Analysis

The levels of gene expression were analyzed using reverse transcription-polymerase chain reaction (RT-PCR). Total RNA in the cultures was extracted using TRIzol (Invitrogen, Carlsbad, CA) and a purification column (RNeasy, Qiagen, Valencia, CA). Following DNase I treatment, 1 µg of total RNA was reverse-transcripted into a cDNA template using MMLV reverse transcriptase (Clontech, Carlsbad, CA) and oligo(dT) primer (Clontech) at 42°C for 1 hour and at 94°C for 5 minutes. The PCR was performed using TaqDNA polymerase (Ex taq, Takara Bio, Madison, WI) to detect α-I type I collagen, osteopontin, and osteocalcin mRNA. The primer sequences and PCR conditions are described in Table 1. Resulting products were visualized on a 1.5% agarose gel with ethidium bromide staining. The intensities of the bands were quantified under ultraviolet light (LAS-3000; FujiFilm, Tokyo, Japan) and normalized with reference to GAPDH (housekeeping gene) mRNA.

Animal Surgery

Five 10-week-old Sprague-Dawley male rats were anesthetized with a 1% to 2% isoflurane inhalation. After the legs had been shaved and decontaminated with a 10% povidone-iodine solution, the distal aspect of the right and left femurs was exposed via skin and muscle incisions. The flat surfaces of the femurs were selected for implant placement. The implant site was prepared 10 mm from the distal edge of the femur by drilling with a 0.8-mm round bur followed by an expansion using reamers ISO 90 and 100. Irrigation using sterile isotonic saline solution was employed for cooling and cleaning. Afterward, 1 implant from group AE1 was placed into the right femur and 1 implant from group AE2 was placed into the left femur. The surgical sites were then closed in layers. Muscle layers were sutured using resorbable suture thread (Chromic Gut; Johnson & Johnson/Ethicon, Somerville, NJ), whereas the skin layer was closed using a combination of wound clips and nonresorbable sutures (Prolene; Johnson & Johnson/Ethicon). All animals recovered without complications and were given water supplemented with sulfamethoxazole and trimethoprim and rat chow ad libitum during the healing process. The protocol for animal surgery was approved by the University of California at Los Angeles Chancellor's Animal Research Committee, and all experimentation was performed in accordance with the United States Department of Agriculture (USDA) guidelines for animal research.

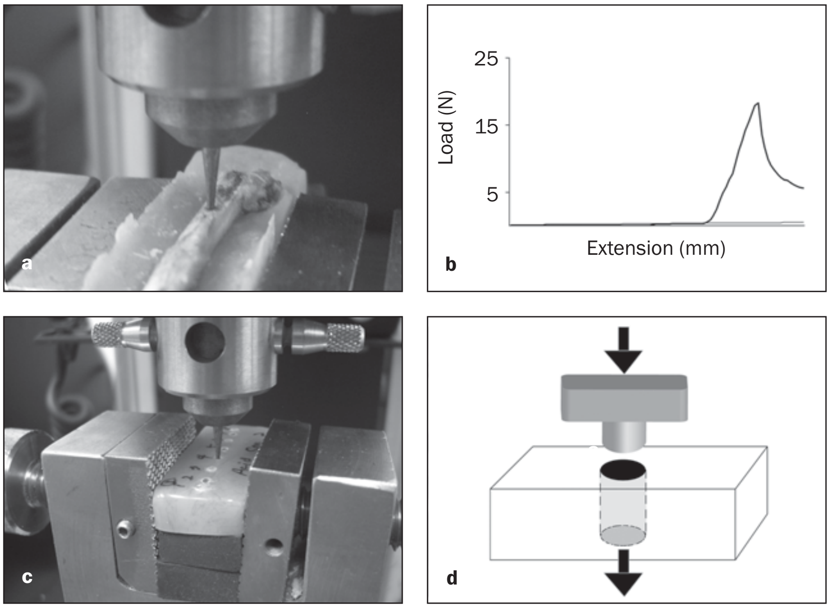

Fig 1 *(a)* Biomechanical strength of osseointegration evaluated by biomechanical push-in test for the 1-step and 2-step acid-etched titanium implants. *(b)* Load displacement curve was registered by an x-y recorder. The peak load to displace the implant was defined as the push-in/ -out value. *(c)* Mechanical retention testing of implants embedded in a resin block. *(d)* Schematic drawing of the mechanical retention testing. The push-out load was applied on the longitudinal axis of the implant.

Implant Push-in Test for Osseointegration Strength

The in vivo anchorage of implants from both groups was examined using a previously established biomechanical implant push-in test in the rat model.[8] Two weeks after surgery, the rats were euthanized in a CO_2 chamber. The femurs were harvested immediately and embedded in a custom-made mold using an autopolymerizing resin. They were sprayed with saline solution every 15 minutes to prevent them from drying. The implant-femur resin block had a flat-bottomed surface that was parallel to the implant platform. Prior to the push-in test, the direction of each implant was measured against 2 axes under an incident microscope (Acoustic Microscope; Olympus Optical, Tokyo, Japan). Afterward, all specimens were tested in a universal testing machine (Instron 5544 Electro-Mechanical Testing System, Instron, Canton, MA) to obtain the push-in values. The testing machine was equipped with a 2000-N load cell that contained a 0.8-diameter custom-made stainless steel pushing rod (Fig 1a). The axial load on the implant was applied at a cross-head speed of 1 mm/min. The maximum error was 0.1 N with a load of 140 N. During constant pushing in, displacement of the implant and the load were recorded simultaneously at a sampling rate of 4 Hz. The load-displacement curve was recorded using x-t recording software (Merlin V5.31, Instron). The push-in test value was determined as the breakpoint load (ie, the maximum load value prior to a rapid decrease in the load-displacement curve; Fig 1b).

Titanium Cylinder Mechanical Retention Test

To investigate the potential impact of AE1 and AE2 surfaces on mechanical implant retention, a push-out test was undertaken with titanium cylinders in a nonbiologic material. A customized mold made from an autopolymerizing resin was prepared. Ten holes with a diameter of 2 mm were made in the resin mold. An autopolymerizing acrylic resin (UniFast II, GC, Tokyo, Japan) was then mixed for 10 seconds and applied to the side surfaces of the 10 cylinders (5 per test group). Afterward, implants were inserted into the holes prepared in the resin mold and allowed to polymerize at 37°C for 24 hours. The titanium specimens were set perpendicular to the horizontal axis of the mold, and the excess resin was removed to expose both ends of each titanium cylinder. Twenty-four hours after specimen preparation, a mechanical retention test was performed by pushing the implants out via the universal testing machine with the aforementioned settings (Figs 1c and 1d). The load displacement curve was recorded using the same software used for the implant push-in test. The push-out value was defined as the maximum load value prior to a rapid decrease in the load displacement curve.

Statistical Analysis

Two-way ANOVA with $P < .05$ as the level of significance was employed to examine differences in cell number variables between the AE1 and AE2 surfaces. The *t* test was applied to determine differences in titanium surface topographies and biomechanical and mechanical retention variables between the 2 surfaces.

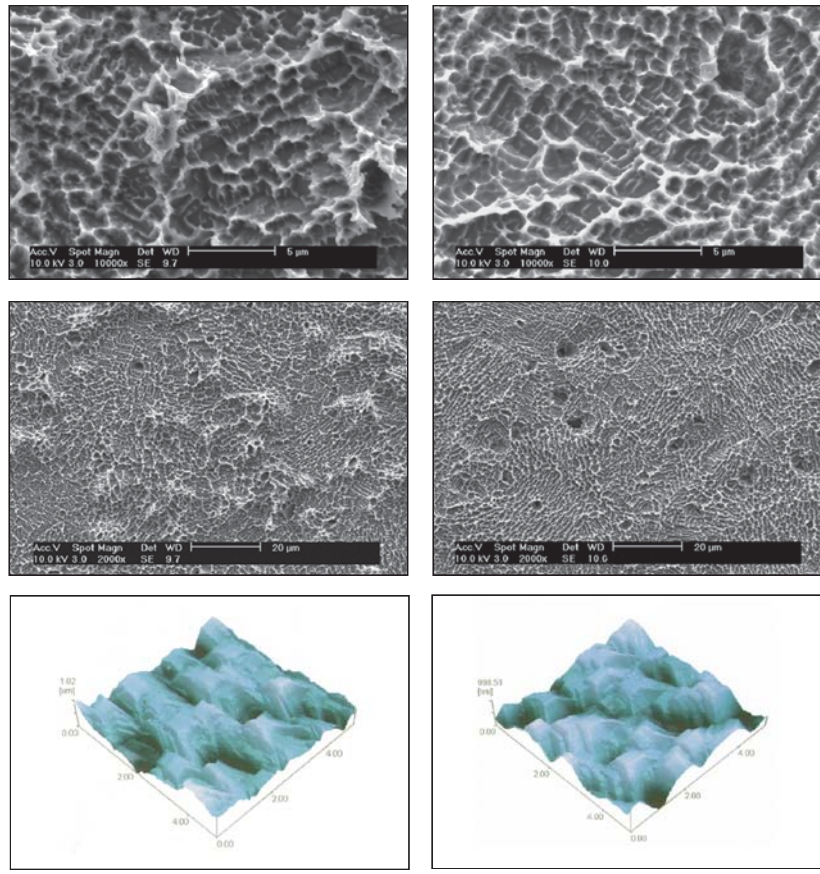

a

b

Fig 2 *(a)* Low- and high-magnification SEM images of the AE1 and AE2 surfaces. *(b)* AFM images of the 2 surfaces. The images were scanned in a 5 × 5-μm area and were constructed in custom vertical scales of 1.02 μm and 0.989 μm for AE1 and AE2 surfaces, respectively. *(c)* Optical interferometer images of the 2 surfaces. *(d)* Elemental spectrum obtained by EDX. *(e)* XRD pattern showing the crystalline structure of the titanium surfaces.

RESULTS

Surface Characteristics of Titanium Samples

The AE1 and AE2 surfaces appeared relatively similar under high-magnification SEM, with uniform micron-scale roughness consisting of compartments 0.5 to 2.0 μm wide with sharp peaks and valleys (Fig 2a). Low-magnification SEM examination, however, revealed differences in the appearance of the 2 surfaces (Fig 2a). Convex structures ranging from 10 to 40 μm in diameter were observed on the AE1 surface but not on the AE2 surface; however, the surfaces were similar with respect to microroughness.

The AFM images of an area of 5 × 5 μm showed a similar 3-dimensional (3D) roughness between the 2 surfaces (Fig 2b). The average roughness (R_a), the root-mean-square roughness (R_{rms}), peak-to-valley roughness (R_{p-v}) and interirregularities space (S_m) were 0.183 ± 0.027 μm, 0.232 ± 0.038 μm, 1.566 ± 0.299 μm, and 1.056 ± 0.297 μm, respectively, for the AE1 surface and 0.188 ± 0.031 μm, 0.235 ± 0.036 μm, 1.356 ± 0.267 μm, and 1.356 ± 0.327 μm, respectively, for the AE2 surface, with no statistical differences between the 2 surfaces ($P > .05$).

Optical interferometry 3D images in an area 1,000 × 1,000 μm revealed that the AE1 had more irregular surface with supramicron scale convexities than the AE2 surface (Fig 2c). The R_a, R_{rms}, R_{p-v}, and S_m values obtained from the optical interferometry were 0.900 ± 0.078 μm, 1.103 ± 0.100 μm, 6.517 ± 0.651 μm, and 68.000 ± 2.345 μm, respectively, for the AE1 surface and 0.605 ± 0.052 μm, 0.746 ± 0.028 μm, 5.475 ± 0.433 μm, and 49.000 ± 5.048 μm, respectively, for the AE2 surface. Statistical analyses showed significant differences in the R_a, R_{rms}, R_{p-v}, and S_m values between the 2 surfaces ($P < .05$). The 2D profile along the cross section of 1,000 μm clearly revealed distinct differences in the configurations of the 2 surfaces, with the AE1 surface depicting a widely oscillating curve indicating the formation of large-scale (supramicron) convexities. The gap between the peaks and valleys of the convex structures ranged 2 μm to more than 7 μm, with the majority greater than 3 μm. The width of the convexities ranged from 10 to 50 μm. In contrast, the 2D profile of the AE2 surface was characterized by a slightly vibrating curve; most of the peak-to-valley gap was less than 2 μm. The density of such convexities was 27.3 ± 5.7 for the AE1 surface and 5.2 ± 3.8 for the AE2 surface ($P < .01$).

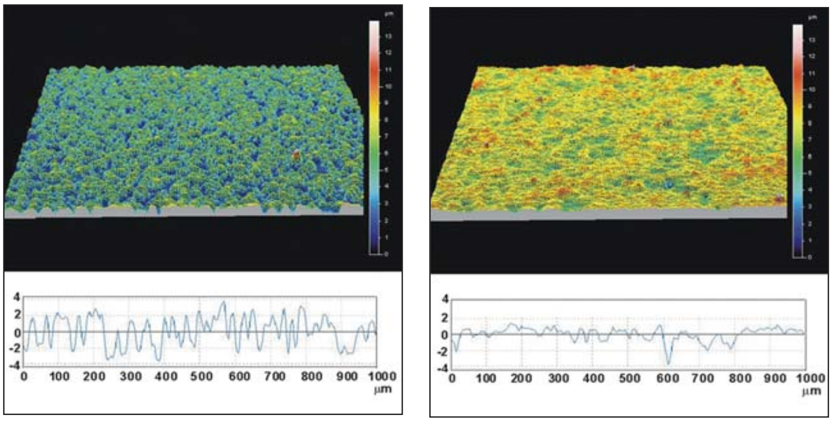

Fig 2 continued *(c)* Optical interferometer images of the 2 surfaces. *(d)* Elemental spectrum obtained by EDX. *(e)* XRD pattern showing the crystalline structure of the titanium surfaces.

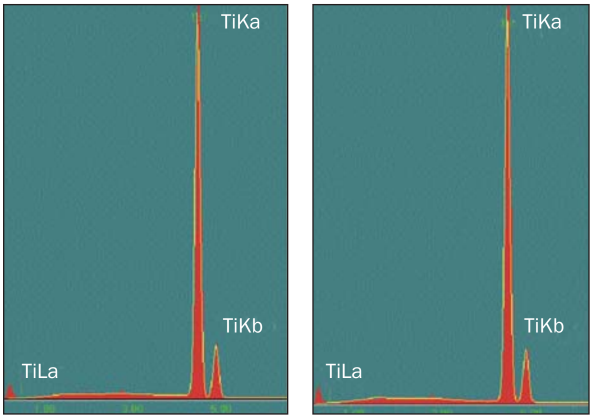

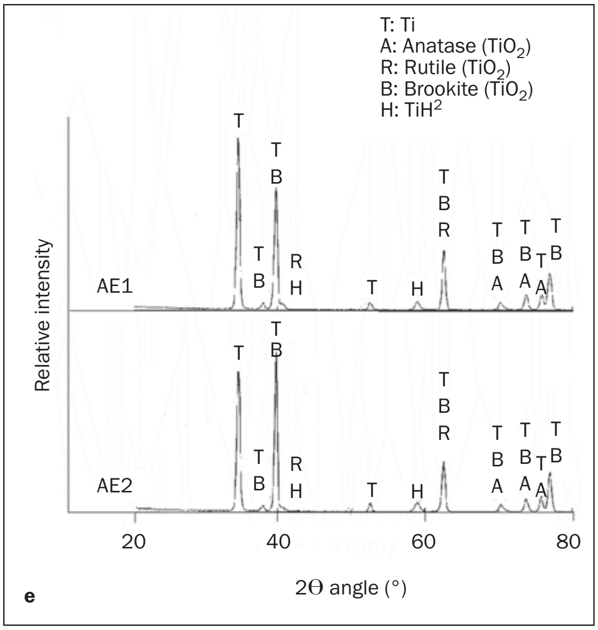

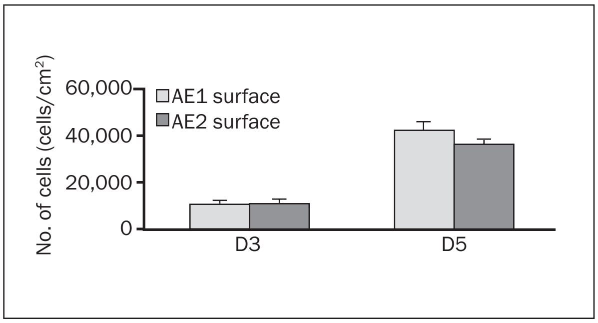

Fig 3 Cell proliferation on the AE1 and AE2 surfaces. Data are shown as means ± SD (n = 3).

The EDX elemental analysis exhibited equally strong titanium peaks for the 2 surfaces without other metallic contamination (Fig 2d). XRD profiling revealed identical peaks of Ti and TiO_2 crystallization on the 2 surfaces (Fig 2e). Higher peak intensity of amorphous Ti and brookite (TiO_2) was observed on the AE2 surface than the AE1 surface at a 2θ angle of 40 degrees.

Cell Density

Compared to culture day 3, the number of cells increased by an average of 3.5 times on both surfaces at culture day 5 (Fig 3). No differences in cell number were found between the 2 surfaces at culture days 3 and 5 ($P > .05$).

Expression of Osteoblastic Genes

The rate of osteoblastic differentiation was examined by determining the expression of osteoblastic marker genes at days 7 and 14. PCR yielded a consistent trend of the amplification, and a representative electrophoresis and the standardized expression level are presented in Fig 4. The expression level of collagen I, osteopontin, and osteocalcin was similar for the AE1 and AE2 surfaces, with no differences greater than 20%.

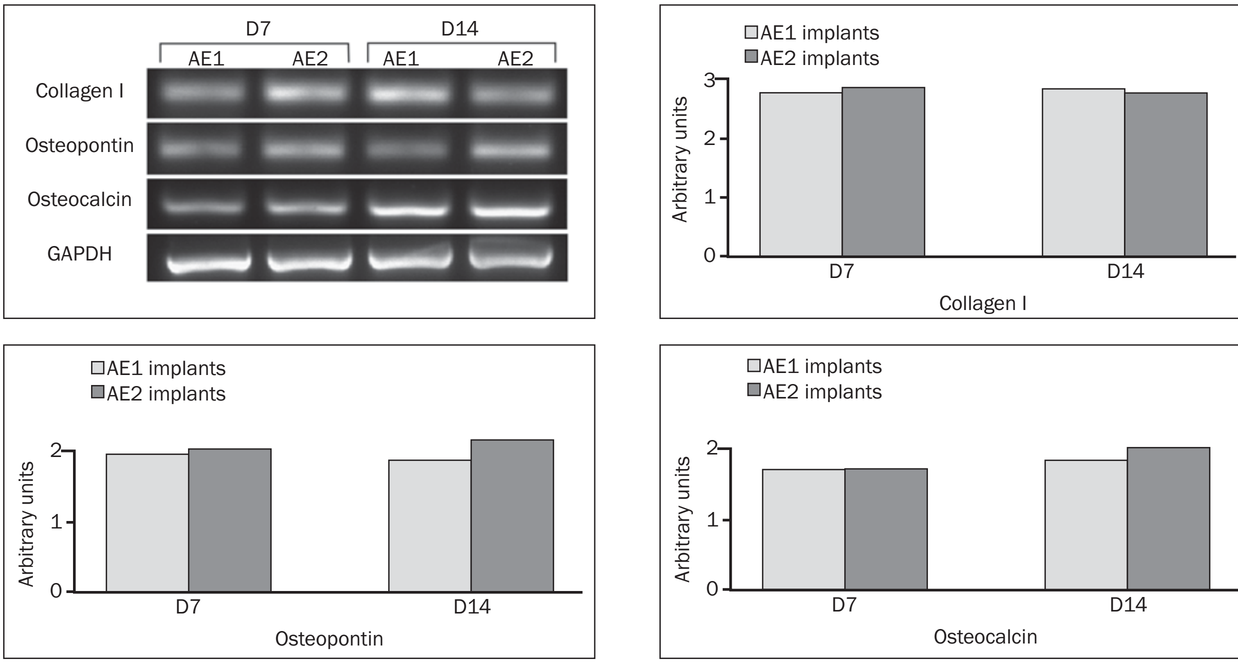

Fig 4 Expression of the bone-related genes in the osteoblastic cultures on AE1 and AE2 titanium surfaces analyzed by RT-PCR. A representative PCR analysis from the PCR amplification, visualized with ethidium bromide staining, is shown. The expression levels of collagen I, osteopontin, and osteocalcin at days 7 and 14 are shown. The intensities of the bands were standardized by GAPDH mRNA expression.

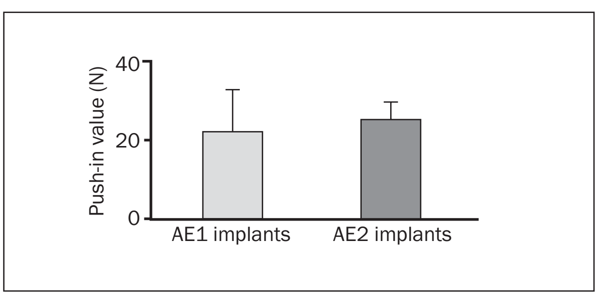

Fig 5 Results of push-in test of AE1 and AE2 implants. The values were obtained at week 2 of healing time. Data are shown as mean ± SD (n = 5).

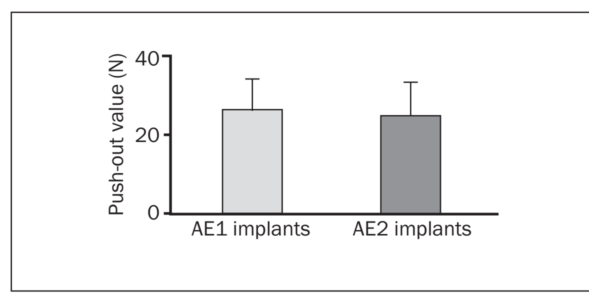

Fig 6 Results of the evaluation of the mechanical retention properties by push-out testing of implants embedded in a resin block. Data are shown as mean ± SD (n = 5).

Biomechanical Strength of Osseointegration

The mean values of the push-in test at week 2 postimplantation were 22.2 ± 10.94 N and 25.4 ± 4.56 N for the AE1 and AE2 implants, respectively, with no statistical difference ($P > .05$; Fig 5).

Titanium Cylinder Mechanical Retention Test

The results of the in vitro push-out test showed mean values of 26.8 ± 7.85 N and 25.4 ± 8.56 N for the AE1 and AE2 groups, respectively (Fig 6). No significant differences ($P > .05$) were found between the 2 surface types.

DISCUSSION

In this study, a variety of in vitro and in vivo tests were carried out to reveal differences in osteoblastic function and in osseointegration phenotypes responding to the titanium surfaces created by 2 different techniques. The 2 surfaces showed similar topographic properties at the micron level of resolution but were distinct at the supramicron level of resolution. For the AE1 surface, 2 topographic configurations were identified by SEM and optical interferometry profiling. The high-frequency topographic property, observed as micron-scale uniformly roughened surface structures, was superimposed on low-frequency topographic structures, which were depicted as interval surface convexities with diameters between 10 and 50 µm. There were apparently fewer surface convexities on the AE2 surface, indicating that the surface has a relatively flat appearance at the supramicron level.

It appears that the treatment with hydrofluoric acid in the AE2 group functions as a pretreatment for the titanium surface, thus eliminating the surface convexities seen on the AE1 surface and transforming the topographic configuration from having both low- and high-frequency structures to having only high-frequency structures. Data obtained from AFM analysis indicated that both acid-etching techniques produced microroughened surfaces. Comparison of the results of the AFM analysis and the optical interferometry evaluation shows differences in the roughness values, which can be explained by the effects of the different measuring equipment used. AFM measures a small area with a very high resolution, while the optical interferometer measures a larger area with a lower resolution. Consequently, the different measurement technologies may lead to different values of surface roughness.[20] Therefore, it is recommended that both small- and large-scale topographic evaluations be carried out to more precisely assess the surface roughness of implants.[20] The elemental composition, which was examined by EDX, was identical between the 2 surfaces and showed dense titanium elemental signals. This indicates that no contamination from the acid-etching treatment was found on either surface. However, the crystal structure of XRD patterns indicated a mixture of anatase, rutile, brookite, and amorphous-type titanium crystals on the AE1 and AE2 surfaces. The peak intensities of different crystals were similar for both surfaces. Several studies have identified different crystallography of titanium oxide surfaces formed with various acids. A mixture of anatase and rutile oxides was identified under wet oxidation using boiling 0.1% H_2SO_4 for 24 hours, while a mixture of anatase and brookite was obtained in boiling 0.2% HCl oxidation for 24 hours.[21,22] The effect of different titanium crystals on its osteoconductive properties is still unclear.

The comparison between AE1 and AE2 titanium surfaces yielded no significant differences in regards to cell proliferation measured by counting the cell number and the rate of differentiation examined by the expression of bone-related gene markers at different time points. Collagen I is known to be an early-stage marker for osteoblastic differentiation, while osteopontin is a mid-stage marker and osteocalcin a late-stage marker. The cellular response to different titanium surfaces has been evaluated in various studies. Obvious or subtle variations in surface topography, as well as differences in surface preparation techniques, make interpretations based on these varying investigations difficult.[18] Nevertheless, microroughened titanium surfaces have been compared to machined surfaces. The former have been found to give advantages over machined surfaces by increasing tissue-titanium mechanical interlocking and promoting osteoblastic differentiation,[23–26] resulting in faster bone formation with less soft tissue intervention.[25,26] In addition, bone integrated to a roughened surface was recently found to be harder and stiffer than bone integrated to a machined surface.[27] However, the bone mass surrounding an integrated roughened implant is smaller than that around machined implant[23] because of the diminished osteoblastic proliferation on microroughened surfaces.[28–30]

The in vivo anchorage quality of implants from both groups was examined using the implant push-in test in the rat model. The push-in test was introduced in a previous study and found to be an effective assay system for evaluation of the biomechanical strength of osseointegration.[8] A healing period of 2 weeks was shown to be sufficient and even more sensitive than a period of 4 weeks to detect differences in the biomechanical strength between implants having different surface topographies or bone metabolic conditions.[8,31] The results of this test supported the in vitro findings, as no significant differences in the push-in data were found between the AE1 and AE2 titanium implant surfaces.

To examine the interfacial retentive capability of the 2 implant surfaces and confirm the results of the in vivo testing, an in vitro push-out test was employed. The effect of bone quality and quantity on the strength of mechanical retention can be excluded in this test because of the use of a nonbiologic material. The results showed no differences between 2 surfaces, thus supporting the in vivo results. It appears that the additional low-frequency topographic property of the AE1 surface enhanced neither the mechanical retention of the implants in the acrylic resin nor the biomechanical retention of implants in vivo.

A majority of studies have shown that a greater degree of mechanical anchorage of bone around microroughened implants is associated with greater bone-titanium contact, when compared to smooth implants.[8,11,12,32,33] It has been claimed that microroughened titanium surfaces with Ra values between 1 and 2 µm provide an optimal surface for bone integration.[16] However, a systematic review on the subject found that a positive effect on the bone response was seen for an Ra value of approximately 0.5 μm to 8.5 μm.[10] few studies have compared the mechanical anchorage of bone around titanium implants with microroughened surfaces created by various techniques. In addition, heterogeneity in study design as well as measurement methods makes interpretations based on these different studies difficult.[10] In an in vivo study, the shear strength of the bone-implant interface for machined and acid-etched (Osseotite) was compared to that of sandblasted and acid-etched implants. Osseotite implants showed mean removal torque values (RTVs) of 62.5 Ncm at 4 weeks, 87.6 Ncm at 8 weeks, and 95.7 Ncm at 12 weeks of healing. In contrast, the sandblasted, acid-etched implants demonstrated mean RTVs of 109.6 Ncm, 196.7 Ncm, and 186.8 Ncm at corresponding times.[34] The authors stated that the significant difference observed in the RTV could most likely be attributed to the different surface characteristics. However, the implants tested in the study differed in macroscopic shape, configuration, and diameter. The possibility that these differences affected the outcome cannot be excluded. In another study, the RTVs of identical solid screw-shaped implants having machined and acid-etched surfaces (MA) and sandblasted and acid-etched surfaces were compared. The results showed that the latter surface was associated with enhanced interfacial shear strength of implants in comparison to the MA surface. RTVs of the sandblasted acid-etched implants were about 30% higher than those of the MA-surfaced implants ($P = .002$), except at 4 weeks, when the difference was at the threshold of statistical significance ($P = .0519$).[17] The authors pointed that slight differences in the surface topography between the 2 implants led to differences in the bone-implant interfacial strength. Although the surfaces tested in the present study were not identical to those in the aforementioned study, the push-in and push-out test results and in vitro osteoblastic responses obtained in this study showed no differences between the 2 micro-roughened surfaces. It appears that the additive supramicron topographic property, as represented in this study by the 10 to 50 μm size convexities with their heights of 3 to 7 μm, does not influence the biological process or the outcome of osseointegration.

CONCLUSION

One-step acid etching produced a surface topography consisting of micro- and supramicron roughness, while 2-step acid etching resulted in a topographic feature of microroughness alone. In vitro osteoblastic function and in vivo biomechanical establishment of osseointegration, as well as the interlocking ability of the surfaces to a nonbiologic material, were not affected by differences between these 2 surfaces.

ACKNOWLEDGMENTS

The authors acknowledge Biomet/3i, Palm Beach Gardens, Florida, and the Japanese Institute for Advanced Dental Studies for partial support of this study.

REFERENCES

1. Albrektsson T, Brånemark P-I, Hansson HA, Lindstrom J. Osseointegrated titanium implants. Requirements for ensuring a long-lasting, direct bone-to-implant anchorage in man. Acta Orthop Scand 1981;52:155–170.
2. Albrektsson T, Jacobsson M. Bone-metal interface in osseointegration. J Prosthet Dent 1987;57:597–607.
3. Albrektsson T, Zarb G, Worthington P, Eriksson AR. The long-term efficacy of currently used dental implants: A review and proposed criteria of success. Int J Oral Maxillofac Implants 1986;1:11–25.
4. Cooper LF. A role for surface topography in creating and maintaining bone at titanium endosseous implants. J Prosthet Dent 2000;84:522–534.
5. Albrektsson T, Wennerberg A. Oral implant surfaces: Part 2—Review focusing on clinical knowledge of different surfaces. Int J Prosthodont 2004;17:544–564.
6. Sykaras N, Iacopino AM, Marker VA, Triplett RG, Woody RD. Implant materials, designs, and surface topographies: Their effect on osseointegration. A literature review. Int J Oral Maxillofac Implants 2000;15:675–690.
7. Davies JE. Mechanisms of endosseous integration. Int J Prosthodont 1998;11:391–401.
8. Ogawa T, Ozawa S, Shih JH, et al. Biomechanical evaluation of osseous implants having different surface topographies in rats. J Dent Res 2000;79:1857–1863.
9. Zhu X, Chen J, Scheideler L, Reichl R, Geis-Gerstorfer J. Effects of topography and composition of titanium surface oxides on osteoblast responses. Biomaterials 2004;25:4087–4103.
10. Shalabi MM, Gortemaker A, Hof MA, Jansen JA, Creugers NH. Implant surface roughness and bone healing: A systematic review. J Dent Res 2006;85:496–500.
11. Klokkevold PR, Nishimura RD, Adachi M, Caputo A. Osseointegration enhanced by chemical etching of the titanium surface. A torque removal study in the rabbit. Clin Oral Implants Res 1997;8:442–447.
12. Buser D, Nydegger T, Oxland T, et al. Interface shear strength of titanium implants with a sandblasted and acid-etched surface: A biomechanical study in the maxilla of miniature pigs. J Biomed Mater Res 1999;45:75–83.
13. Caulier H, Vercaigne S, Naert I, et al. The effect of Ca-P plasma-sprayed coatings on the initial bone healing of oral implants: An experimental study in the goat. J Biomed Mater Res 1997;34:121–128.
14. Vercaigne S, Wolke JG, Naert I, Jansen JA. Histomorphometrical and mechanical evaluation of titanium plasma-spray-coated implants placed in the cortical bone of goats. J Biomed Mater Res 1998;41:41–48.

15. Wong M, Eulenberger J, Schenk R, Hunziker E. Effect of surface topology on the osseointegration of implant materials in trabecular bone. J Biomed Mater Res 1995;29:1567–1575.
16. Albrektsson T, Wennerberg A. Oral implant surfaces: Part 1—Review focusing on topographic and chemical properties of different surfaces and in vivo responses to them. Int J Prosthodont 2004;17:536–543.
17. Li D, Ferguson SJ, Beutler T, et al. Biomechanical comparison of the sandblasted and acid-etched and the machined and acid-etched titanium surface for dental implants. J Biomed Mater Res 2002;60:325–332.
18. Cooper LF, Masuda T, Yliheikkila PK, Felton DA. Generalizations regarding the process and phenomenon of osseointegration. Part II. In vitro studies. Int J Oral Maxillofac Implants 1998;13:163–174.
19. Jokstad A, Braegger U, Brunski JB, Carr AB, Naert I, Wennerberg A. Quality of dental implants. Int Dent J 2003;53:409–443.
20. Wennerberg A, Albrektsson T. Suggested guidelines for the topographic evaluation of implant surfaces. Int J Oral Maxillofac Implants 2000;15:331–344.
21. Koizumi T, Nakayama T. Structure of oxide films formed on Ti in boiling dilute H2SO4 and NaCl. Corrosion Sci 1968:195, 196.
22. Lim YJ, Oshida Y, Andres CJ, Barco MT. Surface characterizations of variously treated titanium materials. Int J Oral Maxillofac Implants 2001;16:333–342.
23. Ogawa T, Sukotjo C, Nishimura I. Modulated bone matrix-related gene expression is associated with differences in interfacial strength of different implant surface roughness. J Prosthodont 2002;11:241–247.
24. London RM, Roberts FA, Baker DA, Rohrer MD, O'Neal RB. Histologic comparison of a thermal dual-etched implant surface to machined, TPS, and HA surfaces: Bone contact in vivo in rabbits. Int J Oral Maxillofac Implants 2002;17:369–376.
25. Ogawa T, Nishimura I. Different bone integration profiles of turned and acid-etched implants associated with modulated expression of extracellular matrix genes. Int J Oral Maxillofac Implants 2003;18:200–210.
26. Takeuchi K, Saruwatari L, Nakamura HK, Yang JM, Ogawa T. Enhanced intrinsic biomechanical properties of osteoblastic mineralized tissue on roughened titanium surface. J Biomed Mater Res A 2005;72:296–305.
27. Butz F, Aita H, Wang CJ, Ogawa T. Harder and stiffer bone osseointegrated to roughened titanium. J Dent Res 2006;85:560–565.
28. Siddhanti SR, Quarles LD. Molecular to pharmacologic control of osteoblast proliferation and differentiation. J Cell Biochem 1994;55:310–320.
29. Alborzi A, Mac K, Glackin CA, Murray SS, Zernik JH. Endochondral and intramembranous fetal bone development: Osteoblastic cell proliferation, and expression of alkaline phosphatase, m-twist, and histone H4. J Craniofac Genet Dev Biol 1996;16:94–106.
30. Owen TA, Aronow M, Shalhoub V, et al. Progressive development of the rat osteoblast phenotype in vitro: Reciprocal relationships in expression of genes associated with osteoblast proliferation and differentiation during formation of the bone extracellular matrix. J Cell Physiol 1990;143:420–430.
31. Ozawa S, Ogawa T, Iida K, et al. Ovariectomy hinders the early stage of bone-implant integration: Histomorphometric, biomechanical, and molecular analyses. Bone 2002;30:137–143.
32. Wennerberg A, Ektessabi A, Albrektsson T, Johansson C, Andersson B. A 1-year follow-up of implants of differing surface roughness placed in rabbit bone. Int J Oral Maxillofac Implants 1997;12:486–494.
33. Masuda T, Yliheikkila PK, Felton DA, Cooper LF. Generalizations regarding the process and phenomenon of osseointegration. Part I. In vivo studies. Int J Oral Maxillofac Implants 1998;13:17–29.
34. Buser D, Nydegger T, Hirt HP, Cochran DL, Nolte LP. Removal torque values of titanium implants in the maxilla of miniature pigs. Int J Oral Maxillofac Implants 1998;13:611–619.